Heat transfer and structural response modelling of FRP confined rectangular concrete columns in fire

Chowdhury, E. U.; Bisby, M. F.; Green, M. F.; Bénichou, N.; Kodur, V. K. R.

Publisher's version / Version de l'éditeur:
https://doi.org/10.1016/j.conbuildmat.2010.12.064
Construction and Building Materials, 25, 12, pp. 1-28, 2011-07-01

Heat transfer and structural response modelling of FRP confined rectangular concrete columns in fire

NRCC-53289

Chowdhury, E.U.; Bisby, M.F.; Green, M.F.; Bénichou, N.; Kodur, V.R.

July 2011

A version of this document is published in / Une version de ce document se trouve dans:
Construction and Building Materials, v. 25, (12), pp. 1-28, July-01-11, DOI: 10.1016/j.conbuildmat.2010.12.064

Heat Transfer and Structural Response Modelling of FRP Confined Rectangular Concrete Columns in Fire

Ershad Chowdhury[a], Luke Bisby[b], Mark Green[a], Noureddine Benichou[c] and Venkatesh Kodur[d]

[a] Department of Civil Engineering, Queen's University, Kingston, ON, Canada
[b] Institute for Infrastructure and Environment, University of Edinburgh, Scotland, UK
[c] National Research Council, Ottawa, ON, Canada
[d] Civil and Environmental Engineering, Michigan State University, East Lansing, MI, USA

Abstract

Fibre reinforced polymers (FRPs) have demonstrated good performance in retrofitting deteriorated reinforced concrete structures. However, there remains a paucity of information on the performance of available FRP strengthening systems at elevated temperatures, and the perceived susceptibility of these systems to fire continues to discourage their use in some applications. To begin to address this issue for the specific case of strengthening rectangular concrete columns with FRP wraps, an experimental and analytical study has been performed. An objective of the study is to develop validated computational models that can be used to perform parametric analyses and suggest design guidelines for these types of structural members. This paper presents the development and partial verification of a computational model that can simulate the structural behaviour of a short or slender, concentrically or eccentrically loaded, unwrapped or FRP wrapped column under both ambient and fire conditions. Results of initial analytical studies, including validation of the model using test data available in the literature, are presented.

Keywords: fire, analytical modelling, FRP, rectangular reinforced concrete, slender column

1. Introduction

Concrete structures can be strengthened using a number of possible configurations of externally-bonded fibre reinforced polymer (FRP) systems in which FRPs are bonded to the exterior of a reinforced concrete member. FRPs have demonstrated good performance in retrofitting and repairing various types of deteriorated concrete structures. However, because of a lack of available information and the widely perceived susceptibility of these systems in fire, an experimental and computational study has been conducted to investigate, both experimentally and computationally, the fire performance of both FRP materials themselves and FRP strengthened concrete structural members. An ultimate goal of the study is to provide rational and holistic fire-safe design recommendations and guidelines for these types of members. This paper presents the development and partial validation of a

computational model that has been developed to simulate the heat transfer and structural response of FRP strengthened rectangular concrete columns in fire.

2. Research Significance

Previous experimental and computational research on the fire performance of FRP confined reinforced concrete columns has focused on the performance of circular members [1, 2]. While these studies have provided a wealth of useful information on the important factors to consider in designing fire protection schemes for FRP confined reinforced concrete columns, the majority of columns in structures are rectangular (or square) and most are subjected to load eccentricities and secondary bending moments. Essentially no information is available on the fire performance of these types of members when strengthened with FRPs. The current paper addresses this considerable gap in knowledge, while also touching on a number of new contributions in related areas; for example structural modelling of slender FRP confined reinforced concrete columns at ambient temperature, and the high-temperature mechanical and bond performance of FRP materials used in external strengthening applications.

3. Computational Model

A computational model was developed and programmed in FORTRAN to predict the temperatures within rectangular reinforced concrete columns (with or without FRP wraps and/or supplemental fire insulation), and this information was subsequently used in a novel fibre-section model to predict their structural behaviour at ambient conditions and during a fire. The overall program logic is shown in Fig. 1. An explicit finite difference method was used to treat the heat transfer analysis within the column, since a similar technique has been widely and successfully used in the past for modelling conventional reinforced concrete structures [3, 4, 5, 6, 7], as well as FRP strengthened reinforced concrete structures [1, 8]. The model for structural behaviour in fire employs a two-dimensional fibre-element analysis and invokes the Column Deflection Curve Method originally proposed by Chen and Atsuta [9]. The model accounts for the temperature-dependent, non-linear thermal and mechanical response of the column's constituent materials, the confining effect of the FRP wraps, and the second-order moments created in an axially-loaded slender column due to lateral deflection.

Initially, all required information is entered as input into the program, including column length and cross-section, steel reinforcement and material details, FRP strengthening properties, and fire characteristics (total duration and user-specified temperature versus time curve).

3.1. Heat Transfer Analysis

The cross-section is discretized into rectangular elements as shown in Fig. 2. The heat transfer from the column's centreline to its exterior surface is calculated using a series of two-dimensional explicit finite difference formulae based on elemental energy balance [4]. The formulation of the finite difference equations and the maximum allowable time step to ensure stability of the algorithm are not included here but are based on work by Lie [4] and Cengel [10]. The variations of the thermal properties of the materials have been included by using relationships described by Lie [4] and Bisby [11]; these are presented in detail by Chowdhury [12]. At any given time step during the analysis, the temperature of any element in the column can be determined based on the temperatures and thermal properties of its adjacent elements from the previous time step. Thus, a complete time history of temperature within the column can be obtained for any prescribed heating scenario.

3.2. Mechanical Property Models at Elevated Temperature

After the temperature distribution of the column cross-section has been determined at each time step, the mechanical properties of the constituent materials are determined at their current temperatures. The compressive stress-strain model proposed by Lie [4] for unconfined concrete was used for the analysis of unwrapped reinforced concrete columns, along with the compressive concrete strength model proposed by Hertz [13] for modelling the mechanical response of concrete at elevated temperatures. The corresponding axial strain at ultimate compressive strength (or peak stress) was described by the model proposed by Terro [14]. It should be noted that research aimed at characterizing the compressive failure (crushing) strain of concrete at elevated temperatures is extremely limited. Williams [15] presented a model describing the unconfined concrete failure strain at elevated temperature, which assumes that the failure strain at elevated temperature is related to the strain at peak stress at elevated temperature by the same stress-to-strain ratio as at ambient temperature. This seems the most reasonable approach in the absence of any specific experimental data, and thus this approach has been implemented in the current model. The transient strain of concrete during heating is dependent on the thermal expansion and the sustained compressive stress experienced by the concrete during heating [16]. The accumulated transient strain for concrete heated under constant stress was modelled by using the uniaxial formula given by Anderberg and Thelandersson [16], which has been successfully used in other research studies [17, 18].

The compressive stress-strain model for FRP confined concrete at ambient temperature proposed by Lam and Teng [19, 20] has been modified in the current study to account for the high temperature deterioration of

material properties using an elastic modulus for unconfined concrete at elevated temperature proposed by Anderberg and Thelandersson [16]. In applying Lam and Teng's [19, 20] model, the average ratio of hoop rupture strain to ultimate axial tensile strain of the FRP material (i.e. strain efficiency) was taken as 0.63 [21].

An elastic-perfectly plastic relationship was used to describe the stress-strain behaviour of the reinforcing steel, both in tension and in compression at both ambient and elevated temperature, based on relationships suggested by Wang et al. [22]. Buckling of the steel reinforcement has therefore not been accounted for in the model.

Since the stress-strain behaviour of the FRP composites at both ambient and elevated temperature was observed to be linear-elastic to failure in direct tension coupon tests conducted by the authors [12, 23], the following equation was used to model the tensile behaviour of the FRP at elevated temperatures:

$$f_{frp}(T) = E_{frpt}(T) \cdot \varepsilon_{frp}(T) \qquad \text{if } \varepsilon_{frp}(T) \le \varepsilon_{frpu}(T) \qquad (1)$$

where, $f_{frp}(T)$ and $\varepsilon_{frp}(T)$ are the current stress and strain of the FRP at temperature; T, $E_{frpt}(T)$ is the tensile elastic modulus at temperature T, and $\varepsilon_{frpu}(T)$ is the ultimate tensile failure strain at temperature T. $\varepsilon_{frpu}(T)$ is calculated using the following equation:

$$\varepsilon_{frpu}(T) = \frac{f_{frpt}(T)}{E_{frpt}(T)} \qquad (2)$$

where, $f_{frpt}(T)$ is the ultimate tensile strength of the FRP at temperature T. A hyperbolic tangent curve proposed by Gibson et al. [24] has been used to describe the high temperature degradation of the FRP's tensile strength $f_{frpt}(T)$ and tensile elastic modulus $E_{frpt}(T)$. The Gibson et al. model is semi-empirical and is based on a non-linear least-squares curve fit of data from tests performed by the authors on a specific glass/epoxy FRP strengthening system at elevated temperatures [12, 23]. The model is described by:

$$f_{frpt}(T) = \begin{bmatrix} \dfrac{f_{frpt}(20\,℃) + 0.46 \cdot f_{frpt}(20\,℃)}{2} \\ -\dfrac{f_{frpt}(20\,℃) - 0.46 \cdot f_{frpt}(20\,℃)}{2} \tanh\left(0.0882 \cdot (T - 47)\right) \end{bmatrix} \qquad (3)$$

$$E_{frpt}(T) = \begin{bmatrix} \dfrac{E_{frpt}(20\,℃) + 0.67 \cdot E_{frpt}(20\,℃)}{2} \\ -\dfrac{E_{frpt}(20\,℃) - 0.67 \cdot E_{frpt}(20\,℃)}{2} \tanh\left(0.1024 \cdot (T - 51)\right) \end{bmatrix} \qquad (4)$$

where, $f_{frpt}(20\,℃)$ and $E_{frpt}(20\,℃)$ are the tensile strength and tensile elastic modulus of the FRP at room temperature, respectively. The FRP was conservatively assumed to be totally ineffective at temperatures above 200°C, again on the basis of material tests performed by the authors [12, 23]. It should be noted that it is likely that

most continuous, unidirectional glass and carbon fibre FRP materials would retain a considerable portion of their tensile strength at temperatures well above 200°C. However, the tests conducted by the authors [12, 23] were limited to a maximum temperature of 200°C and additional testing is needed to more completely understand the response of FRP materials at temperatures up to and exceeding their thermal decomposition temperature. Complete details of the material models used in the current paper are provided by Chowdhury [12].

3.3. Structural Analysis

The objective of the structural portion of the model is to determine the failure load for an eccentrically-loaded column at each time step during exposure to a user-specified fire. This requires the derivation of the moment versus curvature relationship for the column's cross section for increasing axial load levels under heating, followed by calculation of axial load versus maximum moment paths for a given initial load eccentricity and column length. The analysis is based on the following standard assumptions: (1) plane sections remain plane; (2) the total strain in the reinforcement is equal to the total strain in the concrete at the same location; (3) the longitudinal stress at any point in the cross-section is dependent on the longitudinal strain; and (4) the tensile strength of the concrete is negligible.

For each element of the column's cross-section, the stresses and strains are assumed to be those at its central node (refer to Fig. 2). The temperature and strain in the longitudinal reinforcing bars are assumed to be the same as those for the concrete elements that the centroids of the steel bars lie within. Since the FRP wrap is thermally thin and has slightly variable temperature around the perimeter of the column at any given instant during the fire, the mechanical properties of the FRP wrap material are conservatively determined based on the highest temperature achieved by any of the elements at any location within the FRP during a given time step. This is appropriate since the FRP wrap is hottest at the corners, which is where confinement is most activated.

Using an incremental iterative procedure, the moment-curvature response of the column's cross-section for a given axial load is calculated. The stresses and internal forces in the concrete and steel are determined using a two-dimensional fibre-element analysis (refer to Fig. 3). Note that the FRP acts only to confine the concrete and to enhance its ultimate strength and deformation capacity [19]. To derive the moment-curvature relationship, various strain profiles are assumed over the cross-section by incrementally increasing the depth of the neutral axis and the concrete strain at the extreme compression fibre (up to the concrete compressive failure strain at high temperature).

For each proposed strain profile, an axial load and bending moment combination is obtained using two-dimensional fibre-element analysis and then the calculated axial load is compared to the given applied load. The

procedure is repeated by modifying the strain profile until the calculated load is equal to the applied load within a specified tolerance. Once the moment-curvature relationship for a given axial load is determined, the slope and lateral deflection are calculated along the longitudinal height of the column using the Column Deflection Curve method [9]. This numerical integration method is required to account for the effects of secondary bending moments caused by the coupling of axial load and lateral deflection. For each time step, an axial load-moment path for the column is determined by increasing the applied load incrementally. Thus, from these axial load-moment paths at various time steps, the failure axial load versus time of fire exposure can be predicted. Both material (crushing) and global stability (global buckling) failure modes are accounted for in the model.

Unlike circular columns, rectangular columns are only partially confined when wrapped with FRP [25]. In the current analysis, the effectively confined areas have been assumed to be enclosed by four parabolas extending between the rounded corners of the cross section (refer to Fig. 4). A unique aspect of the structural model described herein is that, to account for the partial confinement of a square or rectangular column, the model explicitly calculates the compressive stresses in the concrete elements within the unconfined and confined regions separately, rather than transforming the rectangular section into an equivalent circular section as is done in most procedures for dealing with variable confinement in rectangular columns (e.g. [26] and [19]).

4. Model Validation

The computational model has been validated by comparing its predictions against experimental results presented in the literature [27-31] on both concentrically and eccentrically loaded unwrapped reinforced concrete and FRP strengthened reinforced concrete square columns under both ambient and fire conditions.

4.1. Validation against Unwrapped Reinforced Concrete Columns

The structural model was validated at ambient temperature using results from Luciano and Vignoli [27] on slender, square reinforced concrete columns. Luciano and Vignoli present results from tests on columns made with different types of concrete under varying eccentric loading conditions. The columns had cross-sectional dimensions of 100 mm square and effective lengths of 2120 mm, making them slender according to limits suggested by ACI 318 [32]. Two different reinforcement layouts were used: Column A had four 8 mm diameter longitudinal steel reinforcing bars whereas Column B had four 12 mm diameter longitudinal steel reinforcing bars; both had 6 mm diameter steel ties for transverse reinforcement and both had a concrete cover of 15 mm.

Table 1 and Fig. 5 show a comparison of selected model predictions against the experimental data. Based on this comparison, the model is able to calculate the second-order deformations, the trend of the axial load versus lateral deflection response, the maximum axial load carrying capacity, and the corresponding lateral mid-height deflection at maximum axial load. Fig. 5 also shows the predicted axial load-bending moment strength interaction diagram for these columns; this interaction diagram was also developed using the current model. Because of the high slenderness ratios of the columns in this study [27], they were generally not able to achieve the full strength of their cross sections and thus experienced global stability failures, which were also predicted by the model. This comparison indicates that the model satisfactorily predicts the load carrying capacity and load-deformation response of unwrapped, slender, eccentrically-loaded, rectangular reinforced concrete columns at ambient temperature.

The computational model was also validated by comparison against several experiments presented by Lie and Woollerton [29] on unwrapped square reinforced concrete columns in fire. These tests were on 305 mm square columns which were 3810 mm long and reinforced internally with four 25 mm diameter deformed steel bars in the longitudinal direction and with 10 mm diameter ties at 406 mm spacing with a clear cover of 48 mm to the longitudinal reinforcement. Both carbonate and siliceous aggregate concretes were used to fabricate different column specimens. The columns were tested in a standard column testing furnace under fixed-fixed end conditions and sustained, concentric axial compressive service load. However, because a small eccentricity will always exist in such tests due to imperfections in the column and arising from the loading, an initial small initial load eccentricity of one millimetre was assumed during the structural analysis.

Fig. 6 shows experimental and predicted temperatures within the concrete at various depths and the longitudinal steel temperatures as a function of fire exposure time. The heat transfer model was able to predict the temperatures within the concrete and the steel temperature with reasonable accuracy. The computational model predicted higher temperatures for concrete elements near the fire exposed exterior surface than were observed in the tests, although the prediction became closer to the experimental result as the concrete depth increased. Any minor deviations between the predicted and experimental result may be due to uncertainty as to the exact location of the thermocouples located in the columns and also to the fact that thermally induced moisture migration within concrete, which is well known to occur during fire [33], was not taken into account in the thermal analysis. In the current analysis, the effect of moisture was taken into account by assuming that, in each concrete element, moisture began to evaporate when the temperature reached 100°C and that the temperature remained at 100°C until all the

moisture had evaporated [4]. The model was able to predict the temperatures of the longitudinal steel with reasonable accuracy.

Table 1 and Fig. 7 present selected predicted and observed axial load carrying capacity of the unwrapped square reinforced concrete columns in fire for tests reported by Lie and Woollerton [29]. Table 2 shows that the model is generally conservative, and under predicts the failure time by between 27% and 46%. The conservatism of the current model can likely be attributed to the fact that the model used the ultimate concrete strength model for unstressed concrete as proposed by Hertz [13] to simulate the structural behaviour of a preloaded concrete column under fire condition. Preloaded concrete may be 25% stronger than an unloaded concrete at elevated temperatures provided that the initial compressive stress from the preload is about 25 to 30% of the initial room temperature compressive strength [13]. Hence, the model under predicted the failure time by at least 25% in comparison to the failure time observed by Lie and Woollerton [29] during the fire test. Furthermore, note that the heat transfer portion of the computational model predicted higher temperatures within the column in comparison to the temperatures observed during the fire test [29], which may have also resulted in the conservative of the current model. The current model uses a more precise method to determine the second order lateral deflections of the column in fire based an assumed effective length of 2000 mm obtained from previous research studies (e.g. [34]). The model prediction may therefore be more susceptible to uncertainties with respect to the true effective length of the column during the fire tests because the column's effective length assumed in previous research studies (e.g. [34]) appears to have been calibrated on the basis of the test results rather than assumed from the geometry of the test setup.

The model makes an unconservative prediction for Column LWE3 in Table 2. The reasons for this are unknown, although it should be noted that the observed fire resistance from Lie and Woollerton [29] seems to be inconsistent, both with respect to other tests performed by the authors, and with respect to the typical behaviour of concrete members in fire. Comparing the tested failure time for LWE3, which was made from carbonate aggregate concrete, against the failure time for LWE14, which was made with siliceous aggregate concrete, one would expect LWE3 to perform considerably better. LWE3 had a lower applied load and was constructed from carbonate aggregate concrete, which is widely accepted to have superior fire performance when compared to concrete containing siliceous aggregates. It therefore seems likely that the unexpectedly short experimental fire resistance time for LWE3 in Table 2 may have been the result of an unstated experimental factor, such as spalling of the concrete cover.

Fig. 7 shows model predictions for the variation of axial strength with fire exposure time for columns LWC2 (1 mm initial load eccentricity) and LWE14 (25 mm initial load eccentricity). As already noted, the predicted results are conservative in comparison to the experimental results, both for concentrically and eccentrically loaded members. The model was further used to generate strength interaction diagrams and load-moment path curves for Column LWC2 under both ambient and fire conditions (Fig. 8). Based on these typical results, the column did not experience a reduction in strength of more than 5% due to slenderness effects, and hence it behaved as a "short" column under both ambient and fire conditions according to typical definitions of slender concrete members [22, 32]. This illustrates the ability of the model to include secondary moments in its analysis during fire.

Lie and Irwin [31] present a computational model that uses a finite difference method to calculate the temperatures within a concrete column and load-deflection analysis [35] to calculate the strength of a fire-exposed concrete column. Using this computational model, Lie and Irwin [29] evaluated reinforced concrete column LIC1, which was 305 mm square in cross-section and had similar reinforcement details as in Lie and Woollerton [29] (refer to Table 2). The computational model developed herein was also used to evaluate the strength of LIC1 when exposed to an ASTM E119 [36] standard fire. The results from the model are compared against the test data [31] and against the results obtained from Lie and Irwin's [31] model in Fig. 9. During the fire test column LIC1 failed under a sustained applied load of 1067 kN after 208 minutes. Lie and Irwin's [29] model calculated a failure time of 196 minutes. The computational model described in the current paper predicted failure in 185 minutes. The conservatism of the current model with respect to the test data can be attributed to the factors noted previously. The difference between the prediction from the computational model developed in this paper and Lie and Irwin's model [31] can be attributed to the fact that the Lie and Irwin's [31] model used the ultimate strength model proposed by Lie [4], which was calibrated to simulate the fire behaviour of stressed concrete. The current model also explicitly accounts for the transient thermal strain in the concrete, whereas Lie and Irwin's [31] model accounts only implicitly for creep, and transient strains are not specifically considered.

From the above discussion, it can be concluded that the current model is able to make reasonable predictions of the temperatures within reinforced concrete columns. The structural model is able to satisfactorily capture the trends of the axial load-lateral deflection response of slender, square reinforced concrete columns and to make reasonable and conservative predictions of the load carrying capacity of these types of members in a fire

situation. Demonstrating the above capabilities for unwrapped reinforced concrete columns is a necessary prerequisite to modelling FRP wrapped columns in fire, particularly given the scarcity of fire test data for the latter.

4.2. Validation against FRP Wrapped Reinforced Concrete Columns

Experimental data from Masia et al. [37] and Rochette and Labossière [38] from tests on FRP wrapped square concrete prisms tested under ambient temperature conditions were used to validate the axial strength and axial peak strain predictions of the current model. Comparisons of model predictions and test results is given in Table 3 and Fig. 10; these show that the model was able to predict the axial strength of the FRP confined square concrete prisms with reasonable accuracy. The model was also able to predict the axial compressive peak strain in the concrete at the most compressed fibre with reasonable accuracy when the corner radius of the prism was equal to or greater than 25 mm, i.e. when the corner radius was sufficiently large to produce a confined ultimate strength greater than the maximum axial load capacity of the plain concrete. Deviation was observed between the predicted and the test values of axial peak strain when the corner radius was less than 25 mm. Based on the analysis conducted herein, the corners of the concrete square prisms need to be sufficiently rounded to increase the axial strength from FRP lateral confinement; this is widely acknowledged within the FRP strengthening industry [26]. Providing additional layers of FRP wrap could also increase the axial strength of a square concrete prism when the corner radius of the concrete square prism cannot be increased, although this would not make effective use of the FRP's tensile strain capacity.

The model was further used to predict the behaviour of FRP strengthened reinforced concrete square columns under eccentric axial loads based on tests presented by Tao and Yu [28] under ambient temperature conditions. Tao and Yu [28] tested both unwrapped reinforced concrete and FRP strengthened reinforced concrete slender square columns under axial loading conditions with varying initial load eccentricity. The columns had cross sections of 150 mm square and effective lengths of 3060 mm making them slender according to current code provisions [32]. All of the columns were reinforced with four 12 mm diameter deformed steel bars and 6 mm steel ties spaced at 100 mm on centre and having a clear concrete cover of 15 mm. Two sets of specimens are presented by Tao and Yu [28]; the first set investigating the behaviour of concrete columns wrapped with unidirectional FRP and the second using bidirectional FRP. A corner radius of 25 mm was used and the columns were strengthened by wrapping with carbon FRP. Fig. 11 compares the model predictions against the test results. The model was again able to predict the axial strength of the columns with reasonable accuracy and was also able to calculate the second-order lateral deflections at maximum axial load. Stability failure of a column was established in the model by setting

a failure criterion where the column was assumed to have failed when the axial load-moment path showed a decreasing branch after reaching maximum axial load. Hence, the predicted axial load versus mid-height lateral deflection curves in Fig. 11 do not display post-peak curves as were observed in the tests. Since FRP wraps in the hoop direction do not significantly enhance the flexural stiffness of the column specimens, the eccentrically-loaded FRP wrapped slender columns, whose failure is governed by flexural rigidity rather than crushing strength, showed no significant increase in axial strength from the lateral FRP confinement. Nonetheless, the model accurately captures the axial load versus lateral deflection of the columns and their peak compressive load carrying capacity.

To the knowledge of the authors, only one large scale fire test on an FRP wrapped square reinforced concrete column has ever been reported in the literature. Results of a single fire test on a square FRP-wrapped and insulated concrete column are presented by Kodur et al. [30] and these data were compared against the predictions of the model described herein in an attempt to partially validate the full model's capabilities. Similar to the columns tested by Lie and Woollerton [29], the FRP strengthened 406 mm square reinforced concrete column was 3810 mm long and had similar internal steel reinforcement details. Prior to wrapping the column with FRP, its corners were rounded to a 30 mm radius. The column was confined with three layers of externally-bonded glass FRP wrap in the hoop direction. The FRP had a specified design thickness of 1.3 mm per layer of laminate, a 300 mm overlap in the hoop direction and a 25 mm overlap in the vertical direction, and a tensile strength and elastic modulus of 575 MPa and 26.1 GPa, respectively. Finally, the column was provided with 38 mm of a spray applied cementitious insulation system on the exterior of the FRP strengthening system to protect it from elevated temperatures (refer to Fig. 12).

The FRP strengthened and insulated column was exposed to an ASTM E119 [36] standard fire under sustained compressive service load to failure under fixed end conditions. Fig. 13 presents a comparison between the predicted and observed temperatures at various locations on the FRP and insulation in the column during the fire exposure. The model was able to closely predict the temperatures near the corners of the column during the fire test. However, considerable variation was observed between the predicted and the observed temperatures at the column's side faces. This variation was due to the formation of cracks in the insulation near the centreline of the column's sides. At about 40 minutes into the fire test, flames were observed emanating from vertical cracks that had formed in the insulation; these were due to combustion of the FRP's polymer matrix/adhesive near the cracks. As a result, the temperatures at the middle of the column's side faces were actually higher than at its corners. In the absence of cracking of the insulation, the temperatures near the corners would be expected to be higher than those at the side

faces of the column as shown in Fig. 13. Supported by visual observations and photos taken during the test, a modified analysis was performed using the model by assuming the formation of cracks in the insulation at the middle of the column's side faces (refer to Fig. 14). These results are compared against the experimental result in Fig. 15. After assuming cracks in the insulation, the heat transfer model was able to predict the temperatures in the FRP and insulation reasonably accurately. This result clearly shows that cracking of the insulation is potentially important for accurately predicting the heat transfer in insulated FRP wrapped square reinforced concrete columns.

Fig. 16 presents the predicted axial load capacity of the column with increasing fire exposure time. Also included in this figure are model predictions showing the variation in axial load carrying capacity for an equivalent unwrapped reinforced concrete column and an insulated unwrapped reinforced concrete column. The axial strength of an equivalent unwrapped reinforced concrete column was calculated to be about 9206 kN. After wrapping the reinforced concrete column with three layers of GFRP, the axial load carrying capacity was predicted to be increased only by about 5%, demonstrating that large amounts of FRP are required for axial strengthening of square columns with FRP wraps. Without any insulation, the model predicted that the unwrapped reinforced concrete column would fail under a sustained load of 3093 kN after about 125 minutes of fire exposure. However, the structural performance of the reinforced concrete column (without FRP strengthening) was predicted to be considerably improved by providing external passive fire protection in the form of insulation. Assuming that the insulation remains intact and that there is no crack formation within the insulation for the full duration of the fire exposure, and that the mechanical properties of the FRP wrapping material at elevated temperature can be described using the models discussed previously, the effects of the FRP confinement began to diminish after about 60 minutes of fire, and in about 120 minutes the FRP confinement is predicted to be totally ineffective (note that this in no way implies structural collapse). This is evidenced in Fig. 17, which shows a magnified comparison of the predicted capacity of an insulated unwrapped reinforced concrete column and an insulated FRP strengthened reinforced concrete column (with and without cracking of the insulation assumed during the analysis) during fire exposure. It is evident that the axial load capacity curve representing the FRP strengthened column converges with the axial load capacity curve representing insulated unwrapped concrete column shortly after 120 minutes of fire exposure.

The predicted duration of the effectiveness of the FRP confinement is further reduced when the formation of cracks in the insulation is assumed at the side faces (as occurred during the actual fire test). However, based on the results from the computational analysis, the axial load capacity of the column specimen was about 9000 kN after

being exposed to fire for about 240 minutes, essentially regardless of the effectiveness of the FRP wrap. This clearly demonstrates that loss of the effectiveness of the FRP wrap during fire is not, in and of itself, a reasonable failure criterion to use to define the column's fire resistance time.

During the actual test, due to the sudden loss of insulation at about 250 minutes into the fire test, the concrete cover spalled off the column, thus exposing the longitudinal reinforcement to extreme temperatures. Shortly after spalling of the concrete cover the column failed under the sustained applied load. It should be noted that if the insulation had remained intact it is difficult to see how the column specimen could have failed under the applied load in less than 300 minutes. Regardless of the failure of the insulation, the column tested by Kodur et al. [30] achieved a tested four hour fire endurance rating under its FRP strengthened service load.

Based on the above discussion it can be concluded that the model makes reasonable predictions of heat transfer and load capacity for FRP wrapped square reinforced concrete columns in fire, although additional tests are clearly needed before the model can be considered as fully validated. Furthermore, based on both the test data and the computational modelling, it appears that the FRP strengthening system used by Kodur et al. [30] to strengthen a square reinforced concrete column could maintain its mechanical effectiveness for up to 120 minutes with an adequate amount of robust insulation, and that even if the FRP system effectiveness were lost, the column itself could easily achieve a fire endurance in excess of 4 hours.

5. Fire-Safe Design of FRP Strengthening Systems for Rectangular Columns

The authors have previously made recommendations for the fire-safe design of FRP strengthened reinforced concrete beams and circular columns [39]. These recommendations hold also for the rectangular FRP strengthened concrete columns treated herein. A brief summary of relevant concepts is provided below with reference to Fig. 16.

The main objectives of fire engineering are to prevent the loss of life or injury and property loss during fire [4, 40]. An important aspect of the fire safety strategy for any building is thus ensuring that load bearing structural members have adequate fire resistance to prevent both the spread of fire and localized or global collapse. When retrofitting structural members in buildings with FRPs it is important to consider not only the structural response of the materials but also their performance with respect to flammability, smoke generation, and toxicity [41]. Because the current study is concerned only with structural integrity in fire, no further elaboration is provided on the performance of FRPs with respect to flame spread, smoke generation, or toxicity. The interested reader should consult Sorathia et al. [42] for additional information in this area.

Reinforced concrete members that are designed according to modern design codes [e.g. 32, 43] have ultimate strengths that are considerably greater than the loads that are likely to be acting in the event of a fire [39]; the actual loads on a structural member in fire may be anywhere between about 30% and 60% of its actual ultimate strength. This is demonstrated by considering the traces for "RC" and "Experiment" in Fig. 16, which show the predicted strength and presumed service load on this specific column during fire, respectively. When the unwrapped and uninsulated column "RC" is exposed to fire, its strength drops quite rapidly as a consequence of reductions in its mechanical properties during heating. In this case, the unwrapped and uninsulated column is predicted to fail under the applied load after about 120 minutes of fire exposure. When a reinforced concrete member is retrofitted and strengthened using FRPs, the ultimate strength of the member increases, thus allowing for higher service loads to be imposed on the member. For example, compare lines "Insulated-RC" and "Insulated & FRP-RC" in Figs. 16 and 17, where wrapping with FRPs has increased the load carrying capacity and would therefore allow a higher service load on the member. During an unwanted fire event the ultimate strength of the FRP strengthened member will decrease. If no supplemental insulation is provided on the exterior of the FRP, the contribution of the FRP will be lost almost immediately in fire [44]. If insulation is provided, as for "Insulated & FRP-RC" in Fig. 16 and in the test performed by Kodur et al. [30], then the FRP's contribution is prolonged, although realistically it is difficult to see how this could be preserved for more than 120 minutes even with a large amount of supplemental fire insulation (note that this is speculative since available tests do not allow direct interrogation of the FRP's effectiveness during fire). Perhaps most interesting, however, is the trace for "Insulated-RC" which shows that the unstrengthened but insulated column maintains similar strength to the FRP strengthened column for greater than four hours of fire exposure. This clearly shows that the loss of the effectiveness of the FRP strengthening system during fire is not, in and of itself, a reasonable criterion for failure. Rather, the overall structural member must simply maintain sufficient load carrying capacity to resist collapse, and this can be insured during fire by providing insulation to the existing reinforced concrete column, without needing to explicitly protect the FRP.

By providing an appropriate fire insulation system, the increased strength of the retrofitted reinforced concrete member is maintained for some period of time during a fire (close to 120 minutes in the current example) and at the same time the fire insulation system enhances the fire endurance of the reinforced concrete member. Designers of FRP strengthening systems must therefore ensure that the nominal strength at high temperature should at all times be greater than the strengthened service load on the member, as is now recommended by ACI Committee

440 [26]. However, ACI 440 states that the nominal strength of the member at an elevated temperature may be determined using the guidelines outlined in ACI 216 [45] or through testing. It is worth noting that determining the strength of an insulated reinforced concrete member during fire is in no way a trivial exercise.

In North America, fire endurance of reinforced concrete members is typically determined on the basis of prescriptive design codes (e.g. ACI 216 [41]) instead of on rational design calculations to evaluate the performance of the reinforced concrete member under a wide range of conditions during a fire. These existing prescriptive design codes are not able to assess the fire endurance of insulated reinforced concrete members. The computational model developed in the current study is the only available tool that can easily be used to evaluate both insulated reinforced concrete columns and insulated FRP strengthened reinforced concrete columns in fire.

6. Conclusions

On the basis of the computational modelling described in this paper, and in conjunction with comparisons against available experimental data from both ambient condition and fire tests on FRP strengthened reinforced concrete columns, the following conclusions can be drawn:

- A novel computational model has been developed which can be used to predict various aspects of the thermal and structural response of insulated or uninsulated, unwrapped or FRP wrapped, short or slender, and concentrically or eccentrically loaded reinforced concrete columns both under ambient conditions and in fire.
- The model has been shown to satisfactorily (and in general conservatively) predict both the heat transfer and structural response of unwrapped and uninsulated square reinforced concrete columns in fire and at room temperature conditions, both for concentric and eccentric loads.
- The model appears able to accurately capture the axial load versus lateral deflection of slender FRP wrapped square reinforced concrete columns under both concentric and eccentric loads at ambient temperatures, as well as their peak axial compressive load carrying capacity.
- The model was able to closely predict temperatures near the corners of FRP wrapped and insulated square columns during a standard fire test. However, the model is not able predict the temperatures in these types of members when cracking of the insulation occurs, and this is a potentially important factor for accurately predicting the heat transfer in insulated columns which requires additional research (not only for FRP strengthened structures but for all structures protected with supplemental fire insulation).

- On the basis of the model predictions it appears that the FRP strengthening system used by Kodur et al. [30] to strengthen a square reinforced concrete column could maintain its mechanical effectiveness for up to 120 minutes with an adequate amount of robust insulation, and that even if the FRP system effectiveness was lost the column itself could easily achieve a fire endurance in excess of 4 hours under load.
- The model developed in the current study is the only available tool that can easily be used to evaluate the performance of both insulated reinforced concrete columns and insulated FRP strengthened reinforced concrete columns in fire and to demonstrate compliance with the fire safety requirements of ACI 440 [26] for column strengthening applications.

7. References

[1] Bisby, L.A., Kodur, V.K.R., Green, M.F. Fire endurance of fiber-reinforced polymer confined concrete columns. ACI Structural Journal 2005; **102**(6): 883-891.

[2] Chowdhury, E.U., Bisby, L.A., Green, M.F., Kodur, V.K.R. Investigation of insulated FRP-wrapped reinforced concrete columns in fire. Fire Safety Journal 2007; **42**(6-7): 452-460.

[3] Kodur, V.K.R., Baingo, D. Fire resistance of FRP reinforced concrete slabs. IRC Internal Report No. 758, National Research Council of Canada, Ottawa, 1998.

[4] Lie, T.T. Structural fire protection. American Society of Civil Engineers manual and reports on engineering practice no. 78, New York, NY, U.SA: ASCE, 1992.

[5] Lie, T.T., Irwin, R.J. Method to calculation the fire resistance of reinforced concrete columns with rectangular cross section. ACI Structural Journal 1993; **90**(1): 52-60.

[6] Lie ,T.T., Celikkol, B. Method to calculate the fire resistance of circular reinforced concrete columns. ACI Materials Journal 1991; **88**(1): 84-91.

[7] Lie, T.T., Stringer, D.C. Calculation of the fire resistance of steel hollow structural section columns filled with plain concrete. Canadian Journal of Civil Engineering 1994; **21**(3): 382-385.

[8] Williams, B., Kodur, V.K.R., Green, M.F., Bisby, L. Fire endurance of fiber-reinforced polymer strengthened concrete T-beams. ACI Structural Journal 2008; **105**(1): 60-67.

[9] Chen, W.F., Atsuta, T. Theory of beam-columns, McGraw Hill, Inc, New York, 1976.

[10] Cengel, Y.A. Heat transfer: a practical approach. WCB/McGraw-Hill, 1998.

[11] Bisby, L.A. Fire behaviour of fibre-reinforced polymer (FRP) reinforced or confined concrete. PhD thesis, Department of Civil Engineering, Queen's University, Kingston, Canada, 2003.

[12] Chowdhury, E.U., Eedson, R., Bisby, L.A., Green, M.F., Benichou, N. Mechanical Characterization of Fibre Reinforced Polymers Materials at High Temperature. Fire Technology, accepted May 2009.

[13] Hertz, K.D. Concrete strength for the fire safety design. Magazine of Concrete Research 2005; **57**(8): 445-453.

[14] Terro, M.J. Computational modeling of the behaviour of concrete structures in fire. ACI Structural Journal 1998; **95**(2): 183-193.

[15] Williams, B.K. Fire performance of FRP-strengthened reinforced concrete flexural members. PhD thesis, Department of Civil Engineering, Queen's University, Kingston, Ontario, Canada, 2004

[16] Anderberg, Y., Thelandersson, S. A constitutive law for concrete at transient high temperature conditions. ACI (SP 55-8) 1978; **55**: 187-205.

[17] Thelandersson, S. Modeling of combined thermal and mechanical action in concrete. Journal of Engineering Mechanics 1987; **113**(6): 893-906.

[18] Nechnech, W., Meftah, F., Reynouard, J.M. An elasto-plastic damage model for plain concrete subjected to high temperatures. Engineering Structures 2002; **24**(5): 597-611.

[19] Teng, J.G., Chen, J.F., Smith, S.T., Lam, L. FRP strengthened RC structures. John Wiley & Sons Ltd, West Sussex UK, 2002.

[20] Teng, J.G., Huang, Y.L., Lam, L., Ye, L.P. Theoretical model for fiber-reinforced polymer-confined concrete. Journal of Composites for Construction 2007; **11**(2): 201-210.

[21] Lam, L., Teng, J.G. Design-oriented stress-strain model for FRP-confined concrete. Construction Building Materials 2003; **17**(6-7): 471-489.

[22] Wang, C., Salmon, C.G., Pincheira, J.A. Reinforced concrete design, John Wiley and Sons, 2007.

[23] Chowdhury, E.U., Eedson, R., Bisby, L.A., Green, M.F., Bénichou, N. Mechanical characterization of FRP materials at high temperature, Fire Technology 2010, [In Press, Available Online].

[24] Gibson, A.G., Wu, Y.S., Evans, J.T., Mouritz, A.P. Laminate theory analysis of composites under load in fire. Journal of Composite Materials 2006; **40**(7): 639-657.

[25] Thériault, M., Neale, K.W. Design equations for axially loaded reinforced concrete columns strengthened with fibre reinforced polymer wraps. Canadian Journal of Civil Engineering 2000; **2**(7): 1011-1020.

[26] ACI. ACI 440.2R-08: Guide for the design and construction of externally bonded FRP systems for strengthening concrete structures. Farmington Hills, Michigan: American Concrete Institute, 2008.

[27] Luciano, G., Vignoli, A. Strength and ductility of HSC and SCC slender columns subjected to short-term eccentric load. ACI Structural Journal 2008; **105**(3): 259-269.

[28] Tao, Z., Yu, Q. Behaviour of CFRP-strengthened slender square RC columns. Magazine of Concrete Research 2008; **60**(7): 523-533.

[29] Lie, T.T., Woollerton, J.L. Fire resistance of reinforced concrete columns: Test results. IRC Internal Report No. 569, National Research Council of Canada, Ottawa, ON, 1998.

[30] Kodur, V.K.R., Bisby, L.A., Green, M.F., Chowdhury, E. Fire Endurance of Insulated FRP-Strengthened Square Concrete Columns. 7th International Symposium of Fibre Reinforced Polymer Reinforcement for Concrete Structures (FRPRCS), Kansas City, U.S.A., November 6-9th, 2005.

[31] Lie, T.T., Irwin, R.J. Method to calculation the fire resistance of reinforced concrete columns with rectangular cross section. ACI Structural Journal 1993; **90**(1): 52-60.

[32] ACI. ACI 318-05: Building code requirements for structural concrete. Farmington Hills, Michigan: American Concrete Institute, 2005.

[33] Dwaikat, M.B., Kodur, V.K.R. Hydrothermal model for predicting fire-induced spalling in concrete structural systems. Fire Safety Journal 2009; **44**(3): 425-434.

[34] Lie, T.T., Celikkol, B. Method to calculate the fire resistance of circular reinforced concrete columns. ACI Materials Journal 1991; **88**(1): 84-91.

[35] Lie, T.T., Lin, T.D., Allen, D.E., Abrams MS. Fire resistance of reinforced concrete columns. National Research Council of Canada, Division of Building Research, NRCC 23065, Ottawa, 1984.

[36] ASTM. ASTM E119-01: Standard methods of fire test of building construction and materials. West Conshohocken, PA: American Society for Testing and Materials, 2001.

[37] Masia, M.J., Gale, T.N., Shrive, N.G. Size effects in axially loaded square-section concrete prisms strengthened using carbon fibre reinforced polymer wrapping. Canadian Journal of Civil Engineering 2004; **31**(1): 1-13.

[38] Rochette, P., Labossière, P. Axial testing of rectangular columns models confined with composites. ASCE Journal of Composites for Construction 2000; **4**(3): 129-136.

[39] Kodur, V., Bisby, L.A., Green, M.F. FRP retrofitted concrete under fire conditions. Concrete International 2006; **28**(12): 37-44.

[40] Buchanan, A.H. Structural design for fire safety. Chichester, UK: John Wiley & Sons, Ltd, 2001.

[41] Bisby, L.A., Green, M.F., Kodur, V.K.R. Response to fire of concrete structures that incorporate FRP. Progress in Structural Engineering and Materials 2005; **7**(3): 136-149.

[42] Sorathia, U., Dapp, T., Beck, C. Fire performance of composites. Materials Engineering 1992; September: 10-12.

[43] CSA. CAN/CSA-A23.3-04: Concrete Design Handbook, Canadian Portland Cement Association, Ottawa, Ontario, 2005.

[44] Chowdhury, E.U., Bisby, L.A., Green, M.F., Kodur, V.K.R. Investigation of insulated FRP-wrapped reinforced concrete columns in fire. Fire Safety Journal 2007; **42**(6-7): 452-460.

[45] ACI. ACI 216.1-07: Code requirements for determining fire resistance of concrete and masonry construction assemblies. Farmington Hills, Michigan: American Concrete Institute, 2007.

Table 1. Experimental results from Luciano and Vignoli [27] versus predicted results from the model.

Column specimen	Eccentricity (mm)	Test results		Predicted results	
		Mid-height lateral defl at peak load (mm)	Peak load (kN)	Mid-height lateral defl at peak load (mm)	Peak load (kN)
NSCD-A-8	7	13	297	13	300
NSCD-A-13	13	15	216	13	224
NSCD-A-25	24	26	126	20	130
NSCD-B-8	6	14	327	14	341
NSCD-B-13	12	17	249	14	255
NSCD-B-25	24	30	164	22	160

Table 2. Details of specimens from Lie and Woollerton [29], Lie and Irwin [31], and Kodur et al. [30].

Name	Cross Section (mm × mm)	Steel (%)	Aggregate Type	Moisture Content (%)	Concrete Strength (MPa)	Eccentricity (mm)	Applied Load (kN)	Fire Resistance (mins)	
								Test	Model
LWC2	305 × 305	2.2	Siliceous	0	36.9	1.0 (min)	1333	170	130
LWE14	305 × 305	2.2	Siliceous	0	40.0	24.5	1178	183	125
LWC12	305 × 305	2.2	Carbonate	5	39.9	1.0 (min)	1778	216	170
LWE3	305 × 305	2.2	Carbonate	5	39.9	24.5	1000	181	300
LIC1	305 × 305	2.2	Carbonate	5	36.1	1.0 (min)	1067	208	160
KC	406 × 406	1.2	Carbonate	5	52.0	1.0 (min)	3093	256	>300[a]

[a] Note: Model assumes that the insulation remains uncracked and stays in place for the full duration of the fire.

Table 3. Details of specimens from Masia et al. [37] and Rochette and Labossière [38].

Source	Name	Concrete Strength (MPa)	FRP Type	FRP Thickness (mm)	Specimen size b × h × r (mm)	Peak Axial Strain (%)		Wrapped Strength (MPa)	
						Test	Model	Test	Model
Masia et al. [37]	M1	27.2	CFRP	0.26	100 × 300 × 25	1.76	1.87	51.4	44.8
	M2			0.26	125 × 375 × 25	1.63	1.57	40.5	37.0
	M3			0.26	150 × 450 × 25	1.22	1.37	36.2	31.5
Rochette and Labossière [38]	RL1	42.0	CFRP	0.90	152 × 500 × 5	0.69	0.30	39.5	44.1
	RL2	42.0		0.90	152 × 500 × 25	0.92	1.17	42.4	40.0
	RL3	42.0		0.90	152 × 500 × 38	1.12	1.17	48.9	53.1
	RL4	43.9		1.50	152 × 500 × 5	1.02	0.30	43.9	46.5
	RL5	43.9		1.20	152 × 500 × 25	1.35	1.39	50.9	51.0
	RL6	43.9		1.50	152 × 500 × 25	0.90	1.65	47.9	56.1
	RL7	35.8		1.20	152 × 500 × 25	2.04	1.62	52.3	45.4
	RL8	35.8		1.50	152 × 500 × 25	2.12	1.94	57.6	50.4
	RL9	35.8		1.20	152 × 500 × 38	1.92	1.62	59.4	54.0
	RL10	35.8		1.50	152 × 500 × 38	2.39	1.94	68.7	60.0

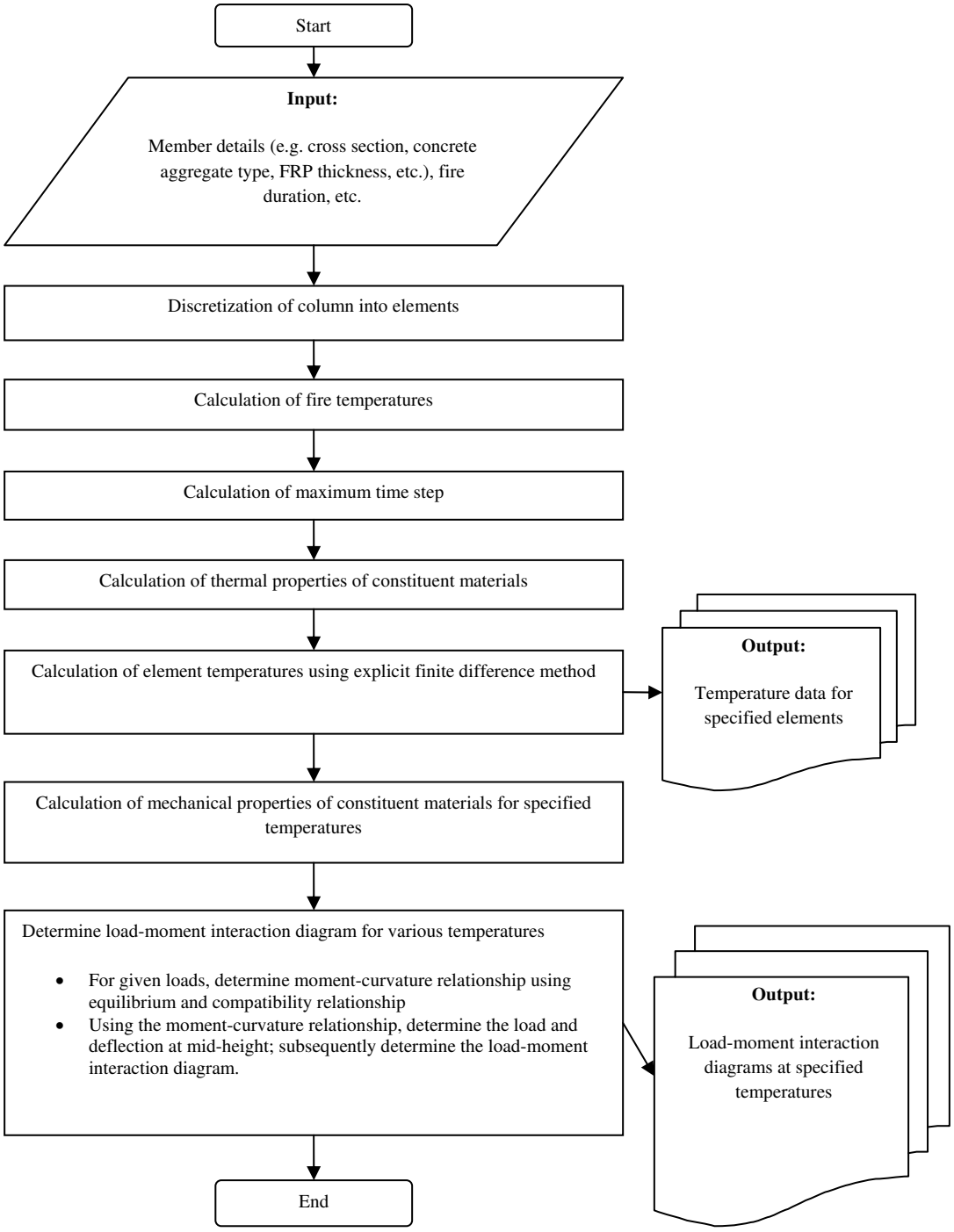

Fig. 1. Flowchart showing the procedures for the fire resistance calculation of columns.

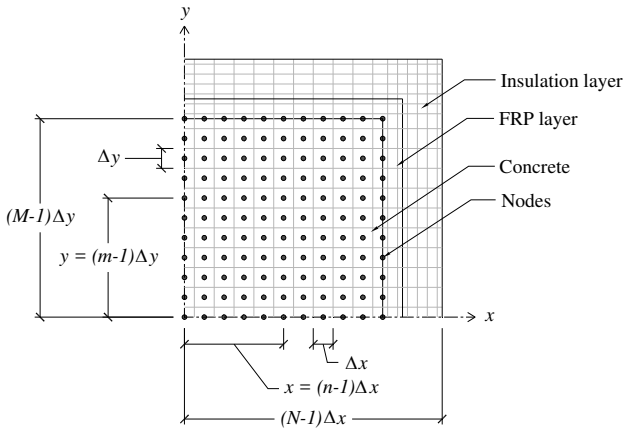

Fig. 2. Discretization of one-quarter cross-section of an insulated and FRP strengthened concrete square column (nodes within the FRP and insulation layer are not shown).

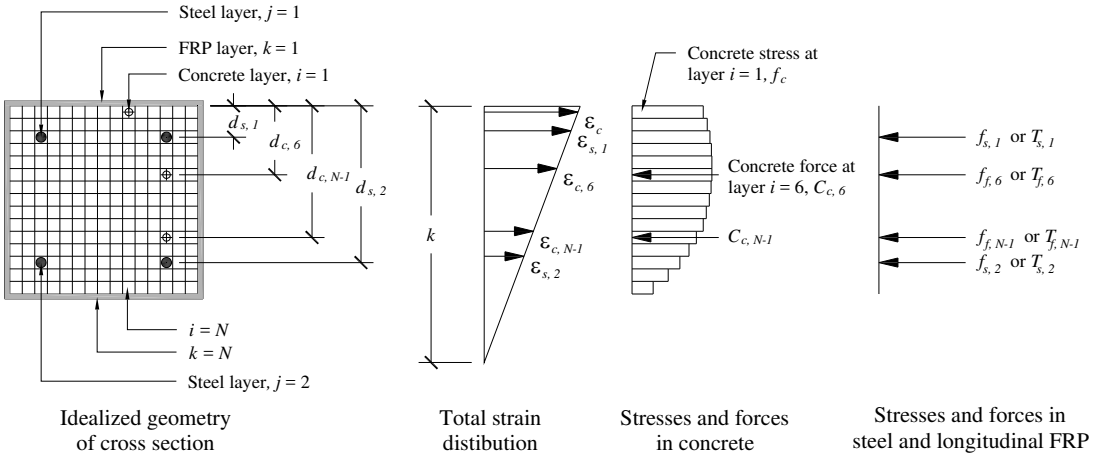

Fig. 3. Two-dimensional fibre analysis for determining the stresses and forces in concrete and reinforcing steel at a given cross-section along the column's height (as required to derive the axial load-moment interaction diagrams and moment-curvature relationship).

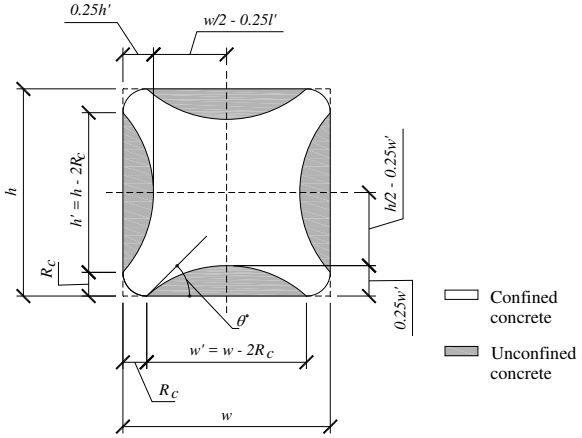

Fig. 4. Assumed effectively confined areas for a rectangular FRP wrapped concrete column [12].

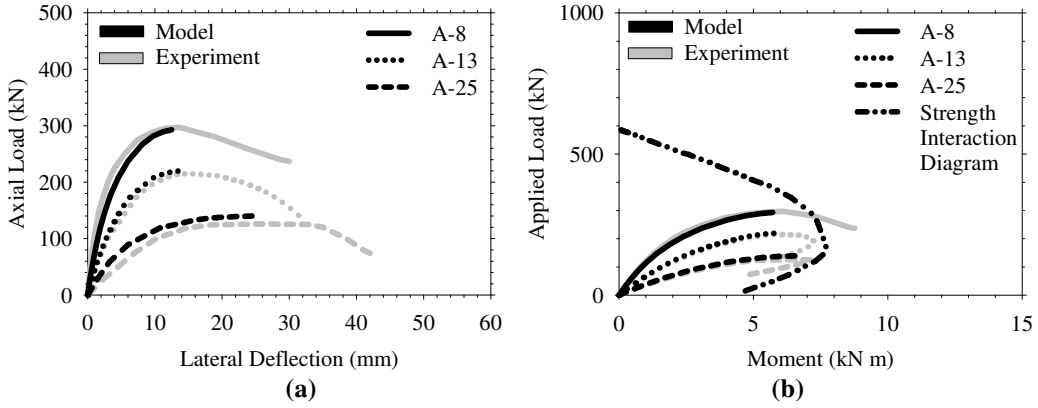

Fig. 5. Predicted and observed (a) Axial load versus mid-height lateral deflection of Column NSCD-A; and (b) axial load-moment interaction diagram for Column NSCD-A (after Luciano and Vignoli [27]).

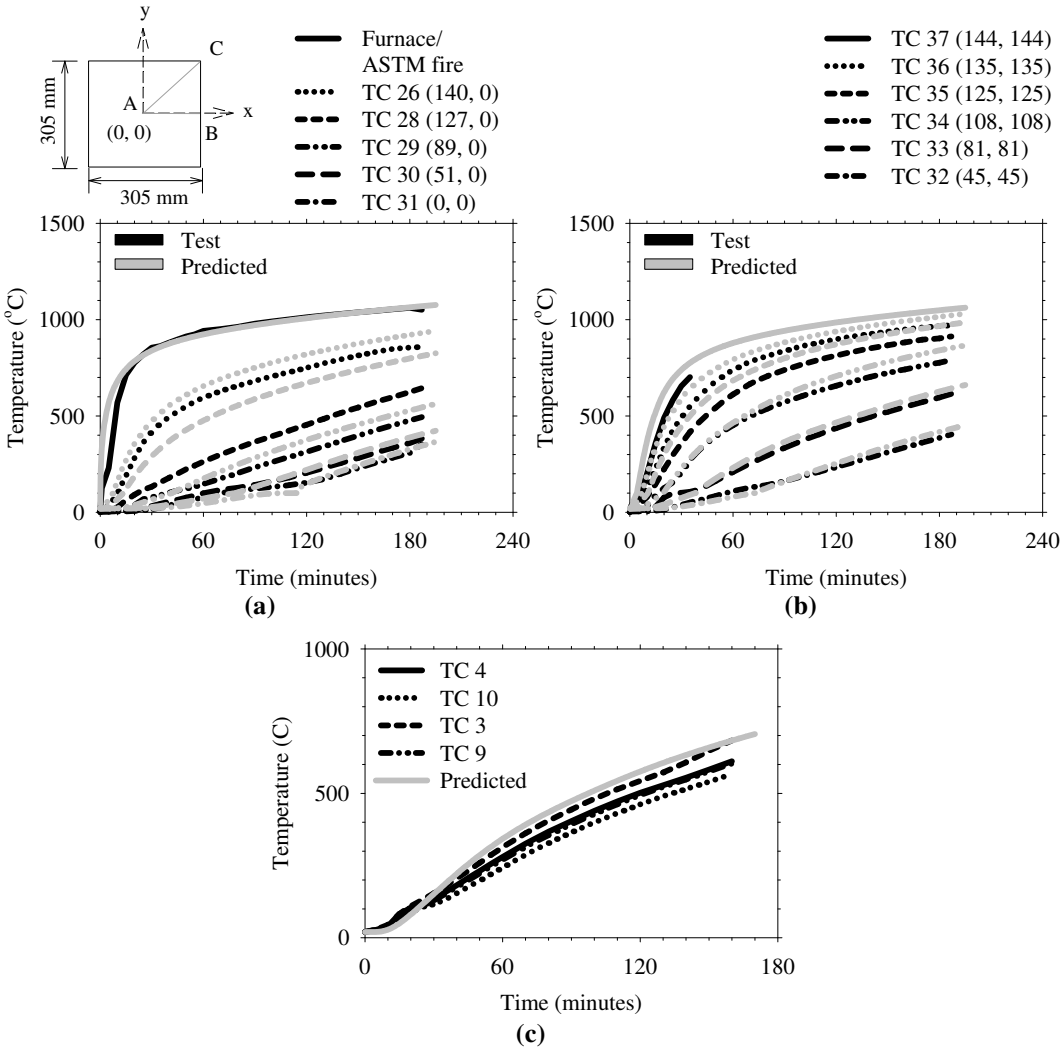

Fig. 6. Variation in concrete temperature within Column LWC9 (a) along the line AB; (b) along the line AC; and (c) on the longitudinal reinforcing steel (after Lie and Woollerton [29]).

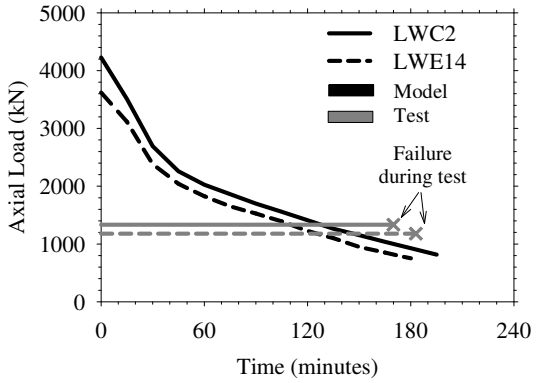

Fig. 7. Predicted axial capacity of unwrapped square reinforced concrete columns LWC2 (1 mm initial load eccentricity) and LWE14 (25 mm initial load eccentricity) in a fire situation for the tests reported by Lie and Woollerton [29].

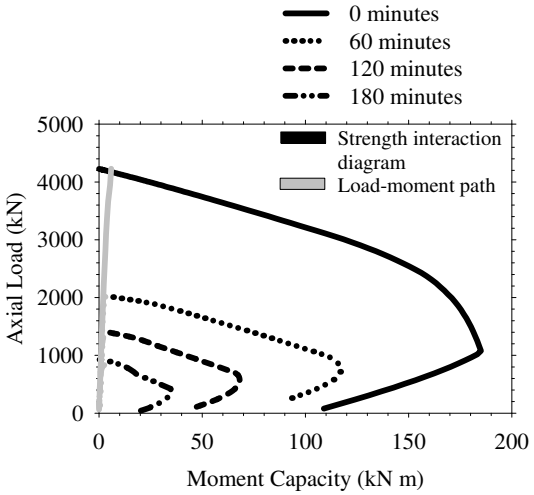

Fig. 8. Predicted axial-flexural strength interaction diagrams for Column LWC2 with increasing fire exposure (after Lie and Woollerton [29]).

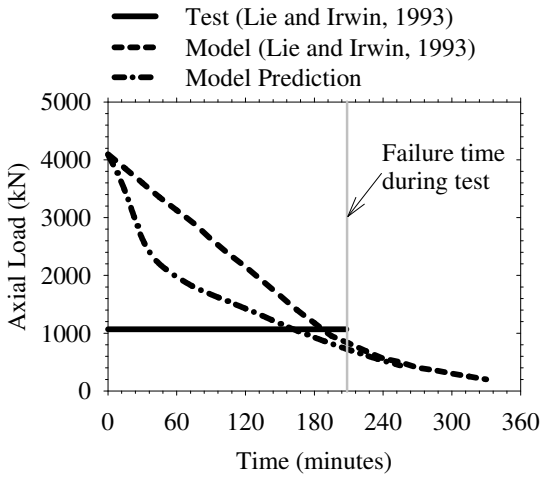

Fig. 9. Predicted variation of axial capacity of siliceous concrete column LIC1 (after Lie and Irwin [31]) with fire exposure time for the current model and the model presented previously by Lie and Irwin [31].

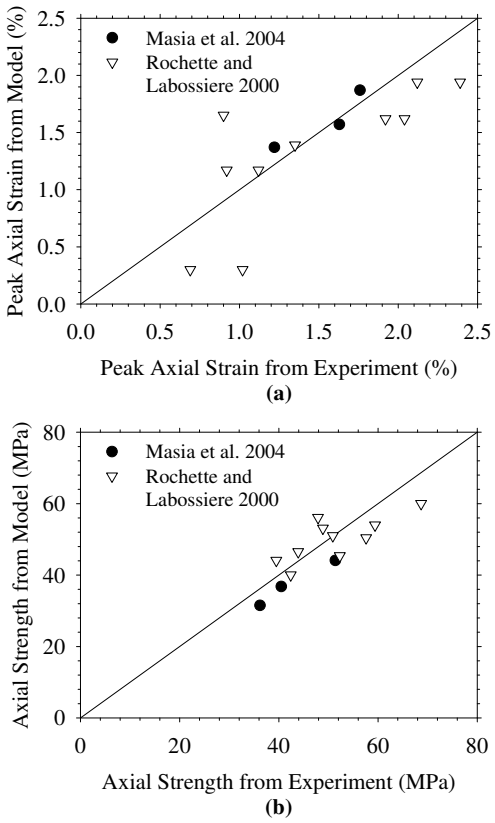

Fig. 10. Performance of the computational model in predicting (a) the peak axial strain and (b) the axial strength of FRP wrapped square concrete prism in comparison with tests.

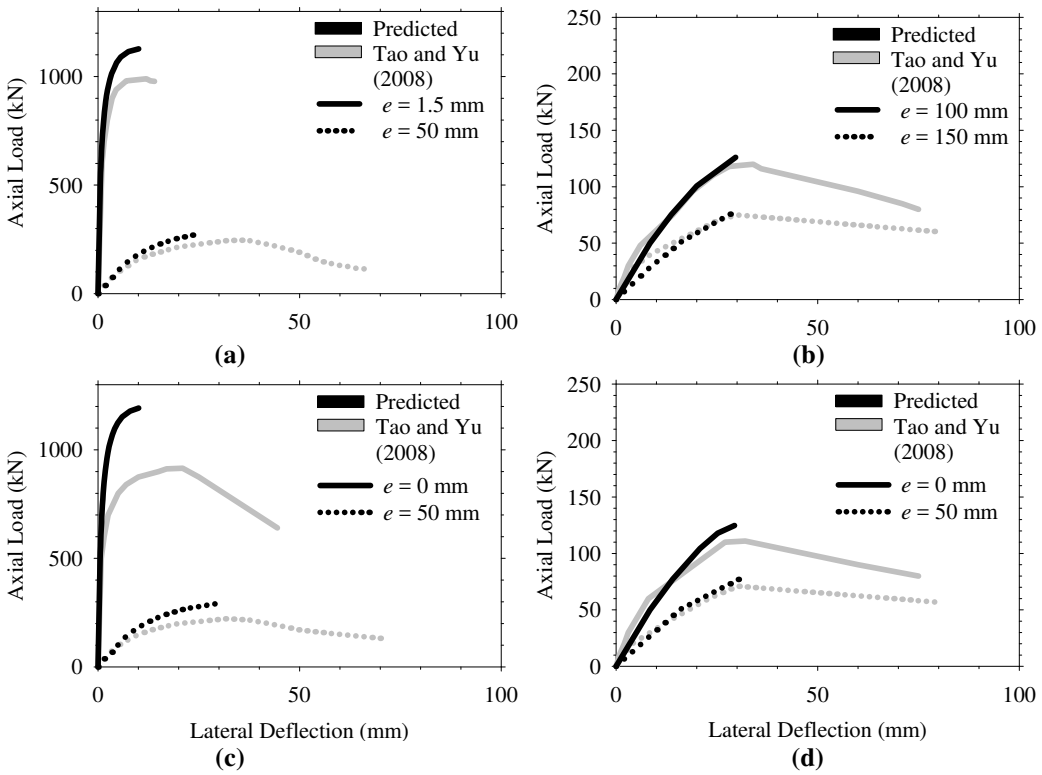

Fig. 11. Predicted and observed axial load versus mid-height lateral deflection of (a) unwrapped reinforced concrete square column specimen (Tao and Yu [28]) having an initial load eccentricity of 0 mm and 50 mm, and (b) 100 mm and 150 mm; and FRP strengthened reinforced concrete square column specimens having and initial load eccentricity of (c) 0 mm and 50 mm, and (d) 100 mm and 150 mm.

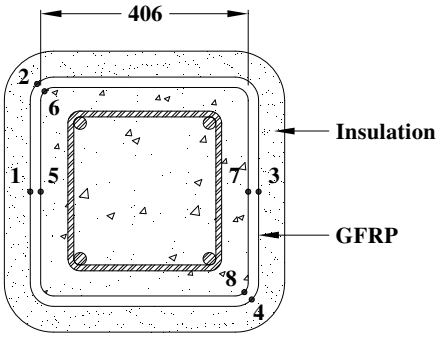

Fig. 12. Thermocouple locations within and cross section of column tested by Kodur et al. [30].

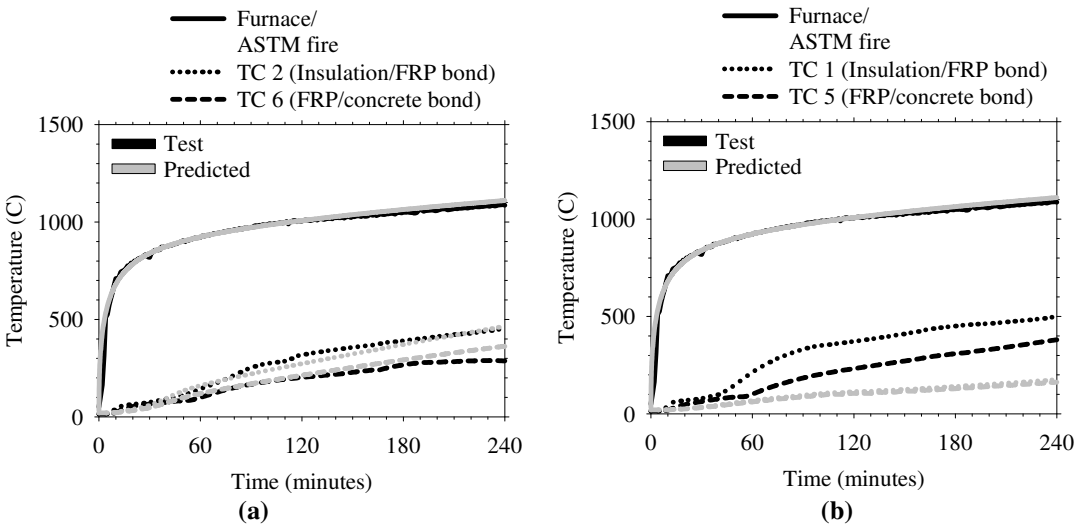

Fig. 13. Predicted and observed FRP and insulation temperatures in the FRP wrapped square reinforced concrete column tested by Kodur et al. [30].

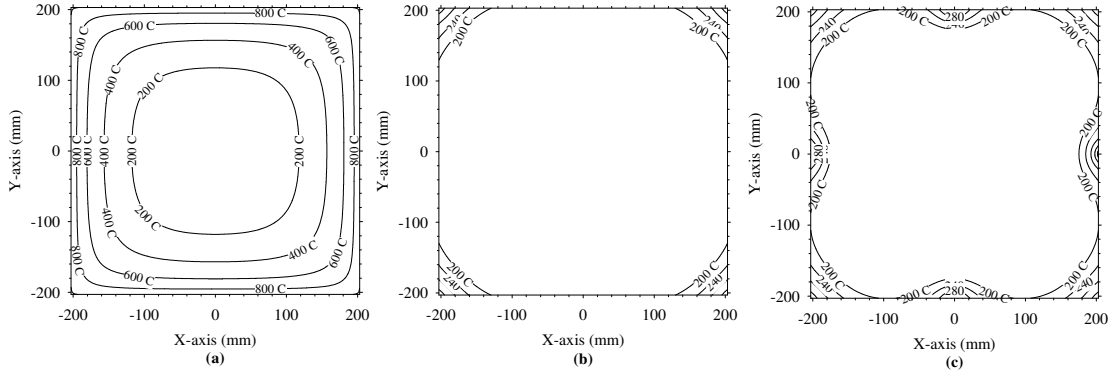

Fig. 14. Temperature distribution of (a) unwrapped reinforced concrete column after 120 minutes of fire exposure, (b) insulated FRP strengthened reinforced concrete column after 240 minutes of fire exposure assuming no cracks within the insulation, and (c) insulated FRP strengthened reinforced concrete column after 240 minutes of fire exposure assuming cracks in the insulation at the centre lines of the column faces.

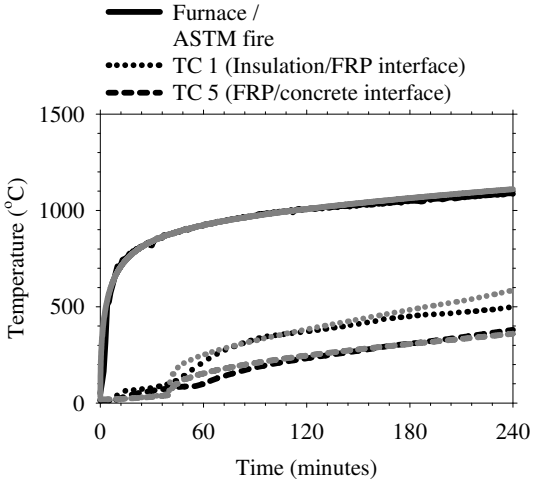

Fig. 15. FRP and insulation temperature on column specimen KC assuming cracks in the insulation.

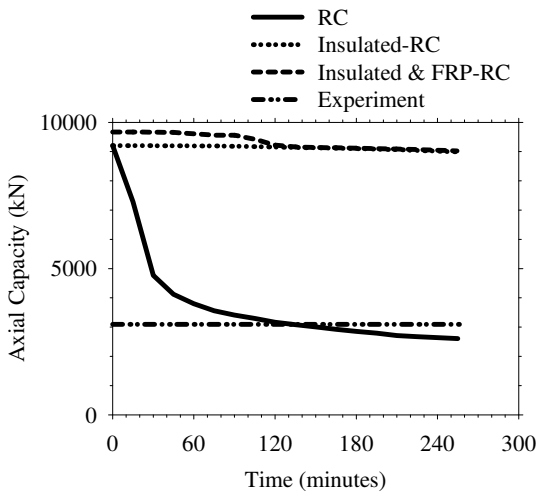

Fig. 16. Predicted variation of axial load capacity of an FRP strengthened reinforced concrete column specimen (after Kodur et al. [30]) with fire exposure.

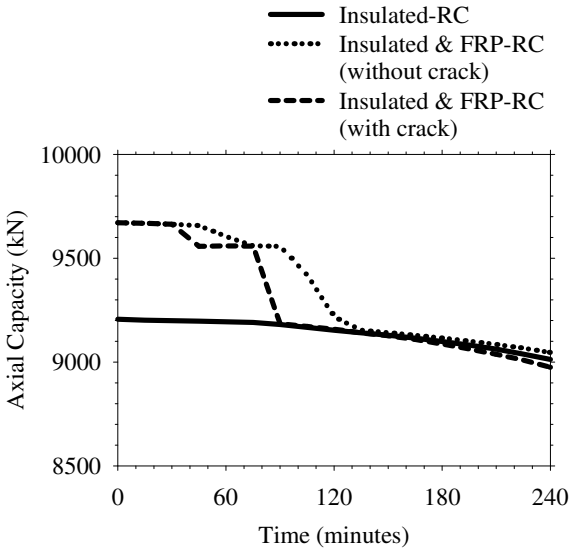

Fig. 17. Predicted capacity of insulated plain reinforced concrete column and insulated FRP strengthened reinforced concrete column (with and without cracking of the insulation) during fire exposure.

List of table captions

List of figure captions